ARTICLE

A study of beam loss pattern and dose distribution around the TPS LINAC during beam commissioning

Ang-Yu Chen[a], Yu-Chi Lin[a,b] and Rong-Jiun Sheu[b,c*]

[a] *National Synchrotron Radiation Research Center, 101 Hsin-Ann Road, Hsinchu Science Park, Hsinchu 30076, Taiwan;* [b] *Institute of Nuclear Engineering and Science, National Tsing Hua University, Hsinchu, Taiwan;* [c] *Department of Engineering and System Science, National Tsing Hua University, Hsinchu, Taiwan*

Beam loss estimation is very important for accelerator shielding design and accurate dose evaluation. The 150-MeV LINAC system of the Taiwan Photon Source (TPS) was assembled and installed in a temporary bunker for acceptance test. Gamma-ray and neutron dose rates around the area were repeatedly measured during beam commissioning. Monitoring results indicated that the beam loss pattern could change drastically over time, especially during the first few weeks of the test, which has caused radiation safety concerns in the area. To facilitate shielding analysis and beam loss diagnosis, FLUKA was used to estimate dose distributions around the area resulting from a series of ideal point beam losses. A full-scale geometry model including main components of the accelerator, structure of the bunker, and additional local shielding has been established to make the simulations as realistic as possible. The resultant dose distributions could be regarded as useful response functions in evaluating combined beam loss scenarios. Taking the beam test on September 23, 2011 as an example, this study has demonstrated that a reasonable beam loss pattern and a detailed dose distribution could be obtained through a synthetic analysis of the calculated response functions and on-site dose rate measurements.

Keywords: LINAC; shielding; Monte Carlo; beam loss pattern; dose distribution

1. Introduction

The Taiwan Photon Source (TPS) in National Synchrotron Radiation Research Center (NSRRC) will soon become one of the most advanced light source facilities in the world [1]. The TPS accelerator system consists of a 3.0-GeV electron storage ring with a circumference of 518.4 m, a concentric booster synchrotron with a circumference of 496.8 m, and a pre-injector of 150-MeV electron LINAC. Due to some delay of the TPS civil construction, NSRRC has built a simple rectangular shielding room made of 1 m thick concrete (called bunker) for the assembly and acceptance test of the outsourcing LINAC. As a pre-injector of the TPS, its operation will generate intense secondary radiation and may present a potential hazard to personnel working in the vicinity of the bunker [2]. During the LINAC commissioning, a series of actions has been carried out to improve radiation safety in the area such as stricter access control and beam interlock, extensive and frequent radiation surveillance, and shielding enhancement. Radiation monitoring indicated that the amount and location of electron losses may change significantly during operations, which have

caused troubles for radiation safety in the area. Gamma-ray and neutron dose rates around the bunker were therefore repeatedly measured and reviewed during that period of time. Because of lacking sufficient beam diagnosis instruments installed along the electron trajectory from the LINAC outlet to the beam dump, radiation survey was also one of supplementary methods providing useful information for beam studies during the LINAC commissioning. More importantly, understanding and establishing the relationship between beam loss pattern and dose distribution is critical in terms of radiation safety since the relationship can have obvious applications in identification of beam loss hot spots and effective installation of local shielding.

2. Materials and methods

2.1. LINAC and radiation measurements

The LINAC is essentially concatenated by three consecutive sections of linear accelerators with a nominal output of 2.25 W (150 MeV, 5 nC, 3 Hz) electron beam. There is a 15 m long transfer line used to guide the accelerated electrons from the LINAC to the beam dump. The lattice function of the transfer line was implemented by four quadruples and a dipole magnet

*Corresponding author. Email: rjsheu@mx.nthu.edu.tw

arranging in an order of Q1, Q2, Q3, D1, and Q4 along the beam trajectory. The dipole D1 was designed to deflect the electron beam horizontally by 10-degree for diagnosis purpose. A dedicated beam dump made of iron core surrounded with lead and polyethylene shielding materials was installed at the end of the transfer line to stop and absorb the beam.

Gamma-ray and neutron dose rates around the test area were constantly monitored from the start of LINAC commissioning. High dose rates up to several mSv h^{-1} outside the shielding room have been recorded occasionally during the initial testing period. The cause for such high dose rates was a mis-steering of electrons and beam losses at unexpected locations. Without proper local shielding to absorb most of the beam energy, stray electrons or bremsstrahlung with sufficient high energies will continue their paths and hit the downstream concrete wall directly. A significant portion of electromagnetic shower will be developed inside the concrete and result in unacceptable high dose rates outside the shielding. To identify and stop similar situations from happening, frequent and comprehensive radiation survey is necessary especially for testing new lattice configuration. In addition to two area monitors installed at downstream and in a lateral direction, respectively, routine survey around the whole area was conducted by using VICTOREEN Model 451P ion chamber for measuring gamma-ray dose rates and using FHT 762 Wendi-2 neutron detector for dose rate measurements.

2.2. FLUKA simulations

To explore the relationship between beam losses and dose distributions, the FLUKA code [3,4] was used to estimate gamma-ray and neutron dose rates around the LINAC area based on a series of simple beam loss scenarios. A rather detailed geometry model including main components of the accelerator, the bunker structure and local shielding arrangement was built aiming to predict practically useful dose rate maps.

Beam loss estimation along the particle trajectory is difficult but crucial for an accurate dose evaluation of accelerators. Due to a lack of reliable beam loss information for the LINAC operation, a series of point beam loss scenarios was assumed for dose distribution calculations. Following the direction of electron trajectory, beam loss locations were respectively assigned at the LINAC outlet, Q1, Q2, Q3, D1, Q4, and the beam dump. Except for the beam dump case, the electron beam was assumed striking the pipe wall at a glancing angle of 1-degree (azimuthally symmetric electron beam) for each scenario. The FLUKA code version 2011.2.6 was adopted to simulate both the development of electromagnetic shower initiated by primary electrons and the subsequent photonuclear reactions induced by secondary gamma rays. Energy cutoffs for electrons and positrons were 100 keV and energy cutoff for gamma rays was 10 keV. Note that no energy cutoff was set for low-energy neutron transport

in the FLUKA simulations. Since the detectors used in NSRRC have been calibrated to deliver ambient dose equivalent H*(10), therefore we chose the built-in fluence-to-ambient dose equivalent conversion factors for dose evaluation.

3. Results and discussion

3.1. Radiation survey and local shielding

During initial beam tests of LINAC, radiation monitoring record indicated that gamma-ray dose rates measured on the outer surface of the downstream shielding wall could possibly reach a level of about several mSv h^{-1}. Compared with the stringent annual dose limit of 2 mSv for personnel in NSRRC, this is unacceptably high and should be rectified before allowing further testing. The reason for causing such high dose rates outside 1 m thick concrete must be related to unexpected beam losses, as explained in Section 2.1. Proper local shielding for beam loss hot spots is the most effective way to reduce the dose rates. The difficulty lies in locating important electron lost points or regions partly because of lacking sufficient beam diagnosis instruments and partly because the beam loss pattern may vary with different operating conditions.

Through repeated tests and radiation survey, we found that placing a lead block at the location between D1 and Q4 for local shielding is very helpful in reducing the dose rates. In addition, a lot of lead bricks were stacked around the entrance of the beam dump to form a better shielding coverage of the hottest core, i.e. the destination of most electrons. With the installation of these local shielding and careful machine tuning, gamma-ray dose rates outside the downstream concrete wall are now mostly below a comfortable level of ~10 µSv h^{-1} during a full-power operation. The neutron dose rates are much lower than that of gamma rays, usually fluctuating around ~0.2 µSv h^{-1} at maximum, which is only slightly higher than its detection limit. Except for the downstream area, gamma-ray dose rates outside the bunker including the roof are well-controlled and approximately below ~1 µSv h^{-1}.

3.2. Beam loss patterns and dose distributions

The current arrangement of local shielding in the LINAC room was mostly based on trial-and-error. This experience motivated us to further examine the relationship between beam loss pattern and dose distribution in the area. Different beam loss assumption may lead to completely different dose distribution. A series of beam loss scenarios with different electron loss locations along the transfer line has been systematically studied by FLUKA simulations. The calculated results confirm the intuitive thought and provide quantitative estimates of the relationship. **Figures 1** and **2** show a good example, where three gamma-ray dose rate distributions are obtained by simulating the primary
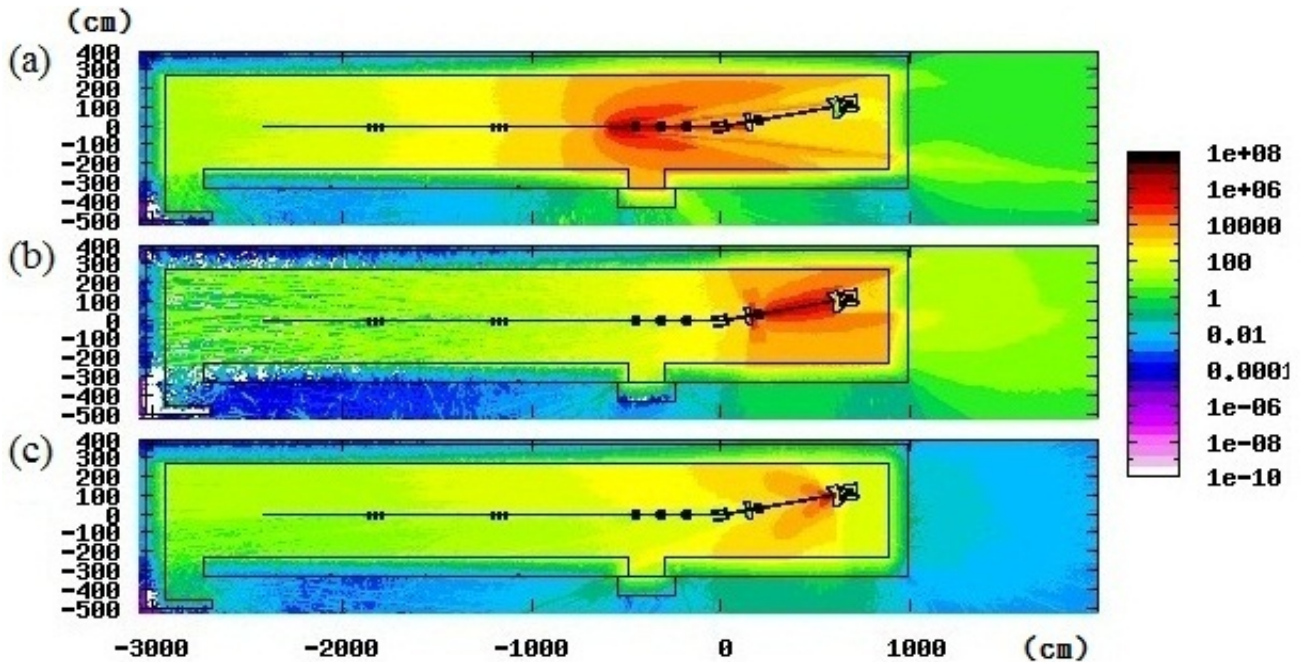
Figure 1.   Gamma-ray dose rate (μSv h^{-1} W^{-1}) distributions around the LINAC area calculated for three beam loss scenarios: (a) electrons lost at the LINAC outlet, (b) electrons lost near the 4th quadrupole, and (c) electrons lost at the beam dump.
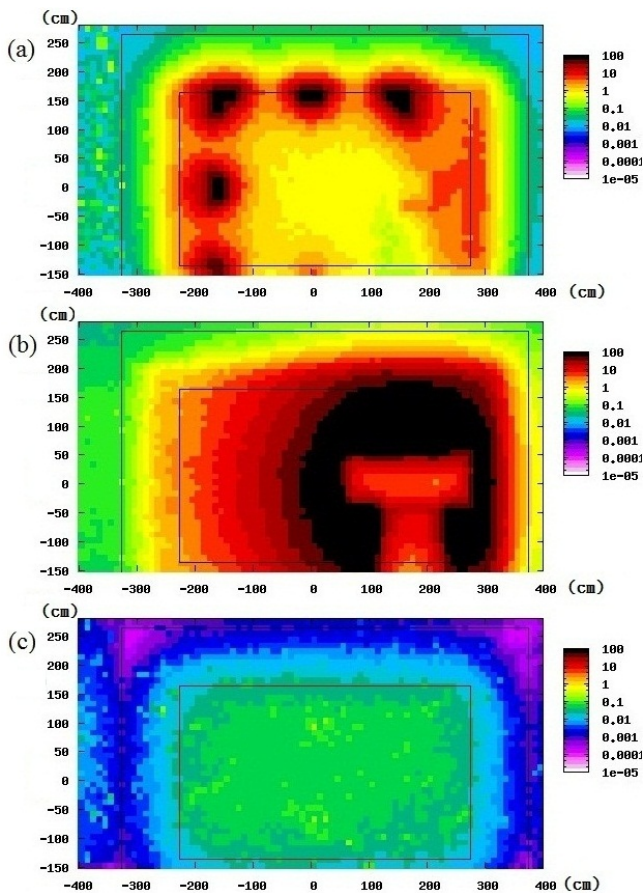

Figure 2.   Gamma-ray dose rate (μSv h^{-1} W^{-1}) distributions on the outside surface of the downstream shielding wall calculated for three beam loss scenarios: (a) electrons lost at the LINAC outlet, (b) electrons lost near the 4th quadrupole, and (c) electrons lost at the beam dump.

electrons lost at three locations, respectively: (a) the LINAC outlet, (b) near the Q4 magnet, and (c) the beam dump. Figure 1 presents a horizontal view of dose rate distributions at the beam level and Figure 2 shows the corresponding dose distributions on the outside surface of the downstream shielding wall where the dose rates are usually the highest during the LINAC operation.

Differences between the resultant dose distributions caused by the three point beam loss scenarios are evident as shown in Figures 1 and 2. It is therefore possible to take advantage of these distinguishing dose patterns in analyzing radiation survey data and their implications. This kind of information (if can be acquired beforehand) is very helpful in beam loss analysis and local shielding arrangement for accelerator operation. For example, in case (c), if all the accelerated electrons are perfectly dumped as designed, gamma-ray dose rates outside the shielding should be quite low, comparable to a natural background level. Obviously, this was not what we have encountered during the LINAC commissioning. On the other hand, cases (a) and (b) in Figure 2 suggest that a small amount of electrons lost at the transfer line is possibly causing meaningful dose rates somewhere outside the downstream shielding wall. Note that their projected dose patterns on the wall are different: case (a) shows scattered hot spots in peripherals; case (b) shows a projected T-shaped shadow on the central high dose rate region.

Beam losses occurred near the last magnet Q4 play a dominant role in the magnitude of downstream dose rates. This observation from Figure 2 is consistent with our finding by trial and error during the commissioning. To better understand the radiation field at the downstream area, **Figure 3** shows the energy distributions of neutrons

and gamma rays scored on the outside surface of the downstream shielding wall for the dominant case (b): electrons lost at Q4. The absolute intensity of neutrons is much lower than that of gamma rays; therefore the neutron spectrum is artificially multiplied by a factor of 1000 to fit in the same scale. The energies of most gamma rays are between 0.1 and 10 MeV. The clear photon peak located at 0.511 MeV resulting from the annihilation of positrons and electrons is one of the characteristics of the radiation field around electron accelerators. Neutrons span a wide range in energy and show two pronounced peaks: one is the Maxwellian distribution of thermal neutrons and the other is peaked at ~2 MeV resulting from giant resonance reactions induced by high-energy gamma rays [2].
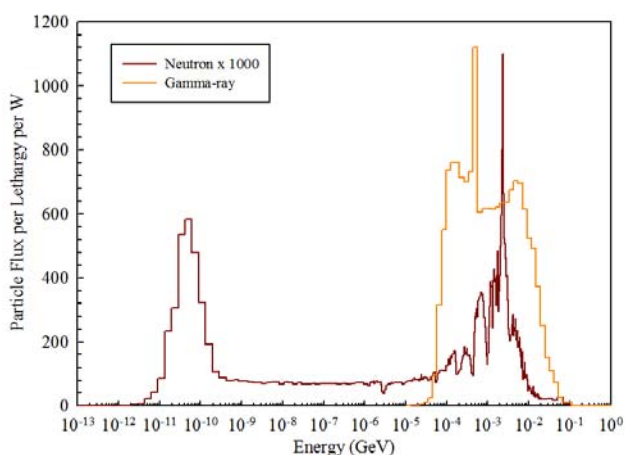

Figure 3. Neutron and gamma-ray energy spectra on the outside surface of the downstream shielding wall for electrons lost at Q4.

3.3. Comparison of calculations and measurements

The dose distributions in Figures 1 and 2 could be regarded as response functions to various beam loss scenarios since they are obtained based on a series of simple point-loss models. To demonstrate the usefulness and applications of these response functions, we analyzed a set of measurement data taken on September 23, 2011. Gamma-ray dose rates were measured at nine positions on the outer surface of the downstream concrete wall during a full-power operation. The measured dose rates are listed in **Table 1** and their respective positions of measurement on the wall are illustrated in **Figure 4**.

During the measurement, fluctuations in detector readings were in a range of about 10-30% because of several constraints and uncertainties, such as time limitation, detector sensitivity, and possible variation of machine operation. Even though the quality of the measured data may not be good, some valuable information could still be extracted from the data with the guidance of the dose response functions shown in Figures 1 and 2. As indicated by electron monitors mounted on the transfer line, approximately more than

95% of the accelerated electrons were successfully dumped into the destination. The beam dump has been designed to contain a full-power electromagnetic shower and to effectively attenuate secondary radiation by using lead and polyethylene. However, measured dose rates were found to be much higher than we previously predicted [5] based on the assumption that all the electrons hit the beam dump. There must be a small portion of beam lost somewhere along the transfer line and causes the unexpected dose rates. The question is how many electrons did not enter the beam dump and where they were lost? Can we have a good estimate of them?

Examining the magnitude and pattern of measured dose rates (Table 1) as well as the calculated dose response functions, we realized that the number of electrons lost at Q4 is sensitive and will dominate the radiation field outside the downstream shielding wall. As a simple guess, we presumed all the accelerated electrons either reaching the beam dump as we wish or being lost by hitting the beam pipe near Q4. Table 1 evaluates this assumption by comparing the estimated dose rates with the measurement. Three similar beam loss scenarios are considered: (i) 1% beam lost at Q4 and 99% beam lost at the beam dump, (ii) 2% beam lost at Q4 and 98% beam lost at the beam dump, and (iii) 3% beam lost at Q4 and 97% beam lost at the beam dump. For 1% beam lost at Q4, the estimated dose rates on the wall are consistently lower than the measurement in most positions. On the other hand, 3% beam lost at Q4 seems a little high compared with the measurement. To the best of our knowledge, the assumption of 2% beam lost at Q4 and 98% beam lost at the beam dump appears to be a most likely scenario for the LINAC operation on September 23, 2011. The overall agreement between the estimated and measured dose rates is satisfactory considering the quality of the measured data and other uncertainties involved in the analysis. Figure 4 shows the resultant gamma-ray dose rate map on the outside surface of the downstream shielding wall calculated for the scenario. This inferred value of 98% beam transfer efficiency from LINAC to the beam dump is consistent with online beam diagnosis data, but not conclusive mainly due to large uncertainties of measuring one-pass electrons.
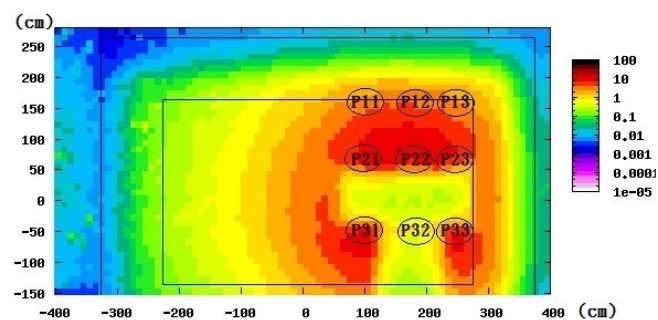

Figure 4. Gamma-ray dose rate (μSv h^{-1}) distribution on the outside surface of the downstream shielding wall calculated for an assumed beam loss scenario (2%Q4+98%Dump). The labels P11-P33 mark the positions of measurement on the wall.

Table 1.   Comparison of calculated gamma-ray dose rates (μSv h^{-1}) with the measurement* (September 23, 2011) at several positions on the outside surface of the downstream shielding wall for three combined beam loss scenarios (1%Q4+99%Dump, 2%Q4+98%Dump, 3%Q4+97%Dump). The measurement uncertainties are estimated to be ~20%.

Position	P11	P12	P13	P21	P22	P23	P31	P32	P33
Measured	2.7	5.3	4.2	2.7	8.3	7.3	11.9	0.3	8.8
1% at Q4	1.8±1.0%	2.3±3.6%	1.6±3.6%	4.1±2.0%	3.7±2.0%	2.8±2.7%	5.1±2.1%	0.3±4.6%	4.1±3.2%
2% at Q4	3.6±0.9%	4.5±3.7%	3.2±3.7%	8.0±2.0%	7.3±2.0%	5.5±2.8%	10.2±2.1%	0.5±5.2%	8.2±3.2%
3% at Q4	5.3±0.9%	6.7±3.7%	4.7±3.7%	12.0±2.0%	11.0±2.0%	8.2±2.8%	15.2±2.1%	0.7±5.4%	12.2±3.2%

* The operating conditions of LINAC were kept constant at about 5 nC, 3Hz, and 150 MeV during the measurement.

4. Concluding remarks

The pre-injector of the TPS is a 150-MeV electron LINAC with a nominal output of 2.25 W. The accelerated electrons are capable of producing intense secondary radiation and causing high dose rates outside the shielding if the electrons are not properly dumped and shielded. Due to a delay of civil construction, the LINAC commissioning was conducted in a simple rectangular bunker made of 1 m thick concrete, in which a dedicated beam dump was designed to terminate the beam and attenuate secondary radiation. Radiation monitoring during the start-up beam test found unexpectedly high gamma-ray dose rates outside the downstream shielding wall. Remedy actions were immediately taken to alleviate the problem including local shielding installation, access control and interlock. The problem was finally understood arising from a small portion of electrons lost near the last quadruple Q4 in the transfer line.

The commissioning experience motivated us to examine the relationship between beam loss pattern and dose distribution around the TPS LINAC in a more systematic way. A series of FLUKA simulations on the dose distribution was performed by assuming various point beam losses along the transfer line. Some resultant dose distributions are distinguishing with each other and can be regarded as response functions, which have been proved to be useful in beam loss diagnosis and analysis of measured dose rates. Using the measurement data on September 23, 2011 as an example, this study has demonstrated that a reasonable beam loss pattern and a detailed dose distribution could be obtained by repeatedly folding beam loss guesses with the response functions and then comparing with measured dose rates. In the case of analysis, an assumption of 2% beam lost at Q4 and 98% beam lost at the beam dump is our best guess on the beam loss scenario judging from the magnitude and the pattern of measured gamma-ray dose rates. This beam loss pattern was somewhat consistent with the result of a quick residual activity survey immediately after ceasing the LINAC operation on Sep. 23, 2011. Beam loss assumption plays an essential role in shielding design and dose analysis of any accelerators. Studying the relationship between beam loss pattern and dose distribution, this work provides a good example of using pre-calculated dose response functions in analyzing field measurement data, from which more detailed and insightful information could be possibly extracted.

References

[1] NSRRC, *Taiwan Photon Source (TPS) Design Handbook*, National Synchrotron Radiation Research Center (2009).

[2] W.P. Swanson, *Radiological Safety Aspects of the Operation of Electron Linear Accelerators*, IAEA Technical Reports Series No. 188, International Atomic Energy Agency (1979).

[3] A. Fassò, A. Ferrari, J. Ranft and P.R. Sala, *FLUKA: A Multi-Particle Transport Code*, CERN-2005-10, INFN/TC_05/11, SLAC-R-773 (2005).

[4] G. Battistoni, S. Muraro, P.R. Sala, F. Cerutti, A. Ferrari, S. Roesler, A. Fassò and J. Ranft, The FLUKA code: Description and benchmarking, *Proc. Hadronic Shower Simulation Workshop* 2006, Sep. 6-8, Fermilab (2006). M. Albrow and R. Raja Eds., AIP Conference Proceeding 896, 31-49 (2007).

[5] R.J. Sheu, J. Liu, J.P. Wang, K.K. Lin and G.H. Luo, Characteristics of prompt radiation field and shielding design for Taiwan Photon Source, *Nucl. Technol.* 168 (2009), pp. 417-423.